

Spin polarized current and Andreev transmission in planar superconducting-ferromagnetic Nb-Ni junctions

E. M. González,¹ A. Domínguez-Folgueras,^{2,3} F. J. Palomares,² R. Escudero,^{1,*}
J. E. Villegas,¹ J. M. González,² J. Ferrer,³ F. Guinea,² and J. L. Vicent¹

¹*Departamento de Física de Materiales, Facultad de CC. Físicas, Universidad Complutense, 28040 Madrid, Spain*

²*Instituto de Ciencia de Materiales de Madrid, CSIC, Cantoblanco, 28049 Madrid, Spain*

³*Departamento de Física, Universidad de Oviedo, 33007 Oviedo, Spain*

(Dated: January 21, 2018)

We have measured and modeled, using three different approaches, the tunneling current in a Nb/Nb_xO_y/Ni planar tunnel junction. The experimental data could be fitted and the correct current polarization could be extracted using a simple quasichlassical model, even in the absence of an applied magnetic field. We also discuss the microscopic structure of the barrier.

PACS numbers: 74.50.+r, 74.80.Fp, 75.70.-i

I. INTRODUCTION

Experiments with tunnel junctions using ferromagnetic metals¹ have been an interesting topic since a long time. This subject has grown again² because of the new field of spintronic where spin dependent currents are an important requisite of many possible devices.^{3,4} This implies that control and measurements of spin polarized currents are needed. Spin-polarized electron tunneling⁵ is a key tool to measure the current polarization and to understand the physics involved in these effects. Most of the recent experimental works have been focused on the suppression of the Andreev reflection and point contact geometry using a superconducting electrode.^{6,7} However the local information extracted by point contact or scanning tunneling microscope techniques seems to be less suitable for devices than planar tunneling junctions. In addition, the intrinsic difficulty of fabricating a perfect uniform oxide layer can jeopardize the latter technique. Recently Kim and Moodera⁸ have reported a large spin polarization of 0.25 from polycrystalline and epitaxial Ni (111) films using Meservey and Tedrows's technique⁵ and standard Al electrode and oxide barriers.

In this work we show that the tunneling electron polarization of ferromagnets could be extracted without applying a magnetic field to the junction and using an oxide barrier with random metallic point contacts. The experimental data are obtained for Nb/Nb_xO_y/Ni planar tunnel junctions. We analyze possible models which describe the experimental results, with emphasis on the information that can be obtained about the shape of the barrier, and the relation between the polarization of the transmitted current and the bulk polarization.

II. EXPERIMENTAL METHOD

Nb(110) and Ni(111) films, grown by dc magnetron sputtering, were used as electrodes. The structural characterization of these films was done by x-ray diffraction (XRD) and atomic force microscopy (AFM), see for in-

stance Villegas *et al.*⁹ Briefly, the junction fabrication was as follows: First, a Nb thin film of 100 nm thickness was evaporated on a Si substrate at room temperature. An Ar pressure of 1 mTorr was kept during the deposition. Under these conditions, the roughness of the Nb film, extracted from XRD and AFM, is less than 0.3 nm⁹ and superconducting critical temperatures of 8.6 K are obtained. After this, the film was chemically etched to make a strip of 1 mm width. A tunnel barrier was prepared by oxidizing this Nb electrode in a saturated water vapour atmosphere at room temperature.¹⁰ Fig. 1 shows the x-ray diffraction data (open circles) of a Nb oxidized film. The thickness of the oxide layer was deduced after the simulation of the data (solid lines) using the SUPREX program.¹¹ It can be seen that the oxide film thickness is 2.5 nm. X-ray photoelectron spectroscopy analysis performed in these oxidized films reveals that dielectric Nb₂O₅ is the main oxide formed, as can be seen in Fig. 2. There are also other oxides, such as metallic NbO, but in much less amount. Taken into account Grundner and Halbritter studies,¹⁰ Nb₂O₅ is the outermost oxide layer on Nb, whereas NbO is located closer to the Nb film. The characterization by AFM reveals a RMS roughness of around 0.7 nm.

On top of this film (Nb with the oxide barrier), the second electrode of Ni was deposited under the same conditions as Nb (up to 60 nm thickness) using a mask to produce cross strips of 0.5 mm width, so that the overlap area S of the two electrodes is 0.5 mm².

Perpendicular transport (tunneling configuration) was investigated by means of characteristic dynamic resistance (dV/dI) versus voltage (V) using a conventional bridge with the four-probe method and lock-in techniques. The measured lock-in output voltage was calibrated in terms of resistance by using a known standard resistor.

Experimental data (open circles) in Figs. 3, 4 and 6 show the behavior of the normalized conductance $G(V)/G_n$ versus the bias voltage V . Conductance has been calculated as the inverse of the differential resistance dV/dI and the normalization has been done with respect

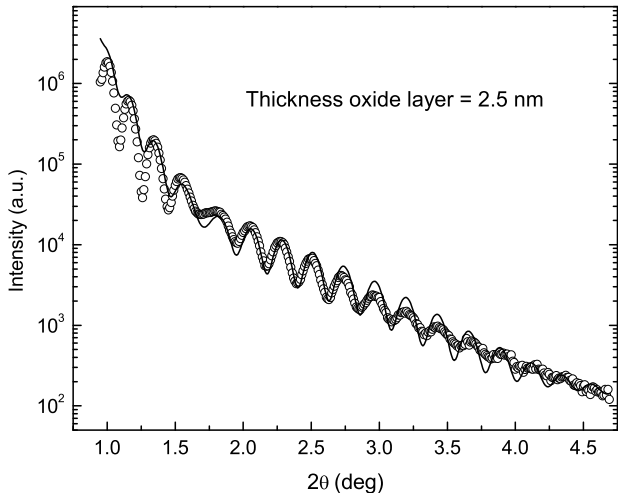


FIG. 1: Measured (open circles) and simulated (solid line) low-angle x-ray diffraction profiles of a Nb film oxidized in a saturated water vapour atmosphere. The thickness of the oxide layer is 2.5 nm, as extracted from the simulation.

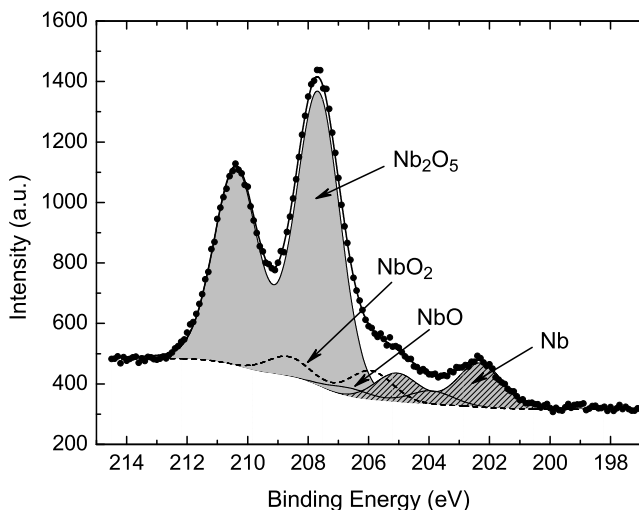


FIG. 2: X-ray photoelectron spectroscopy analysis of a Nb film oxidized in a saturated water vapour atmosphere. Notice that the highest contribution component oxide comes from Nb_2O_5 .

to the dependent voltage background conductance G_n .

III. THEORETICAL DESCRIPTION

A. Introduction

Conductance G across a normal-superconducting junction may be expressed as a function of applied voltage V in terms of the reflection coefficient R of electrons travers-

ing the junction as

$$G(V) = 2 e^2 v_F N_F S \int d\epsilon (1 + A - R) \frac{df(\epsilon - eV)}{d\epsilon} \quad (1)$$

where $f(\epsilon)$ is the Fermi function; v_F and N_F , the Fermi velocity and density of states at the Fermi level, respectively; and A is the coefficient for Andreev reflection processes whereby an electron with energy smaller than the gap impinging onto the junction picks an electron of opposite spin to form a Cooper pair inside the superconductor, leaving behind a hole. Andreev reflection processes are proportional to the square of the conventional transmission coefficient of the barrier T , and therefore are strongly suppressed for highly resistive barriers. Junctions with transmission coefficients smaller than about 0.1 show small subgap conductances.

Our experimental results, shown in Fig. 3, exhibit a significant conductance below the superconducting gap even at the lowest temperatures. Therefore we expect that our effective oxide barriers should be neither too high nor too thick.

We have used three models to describe the transmission across the oxide barrier: i) The simple generalization of the Blonder-Tinkham-Klapwijk (BTK) model¹² to ferromagnetic electrodes proposed by Strijkers and coworkers;¹⁴ ii) a generalization of the BTK model to ferromagnetic electrodes with finite bulk magnetization; and iii) a description of the effects of a finite current polarization in terms of spin dependent transmission coefficients, in a similar way as discussed by Pérez-Willard *et al.*¹⁵.

B. Strijkers' model (Model I)

Strijkers' model uses as adjustable parameters the current polarization

$$P_c = \frac{G_{\uparrow}(0) - G_{\downarrow}(0)}{G_{\uparrow}(0) + G_{\downarrow}(0)}, \quad (2)$$

the height of the barrier Z , which is modeled by a delta function, and the size of the superconducting gap at the interface Δ . The process of electron transfer across the junction is split into a fully polarized channel, for which the Andreev reflection is zero, and a paramagnetic channel described by the BTK model in its usual form. The total conductance is then written in terms of the conductance of the fully polarized channel (G_P) and the conductance of the paramagnetic channel (G_N):

$$G(V) = (1 - P_c) G_N(V) + P_c G_P(V), \quad (3)$$

This model interpolates between the paramagnetic case (BTK model), and the half metal, where it predicts correctly that the amplitude for Andreev reflection vanishes.

The best fit obtained with this model is shown in Fig. 3. The parameters used are $\Delta = 1.4$ meV (superconducting gap), $Z = 1.15$, and $P_c = 0.03$. This value of the

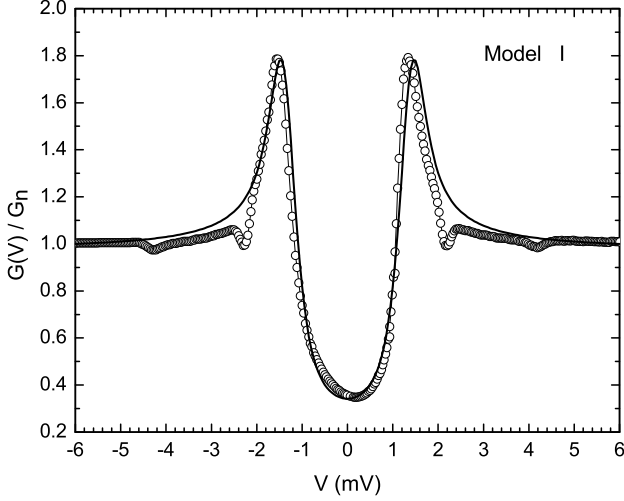


FIG. 3: Normalized tunneling conductance as a function of voltage of a Nb-Ni planar junction. Symbols correspond to experimental data and continuous solid line to the calculated curve using Model I. The temperature of the experiment was 1.52 K and the fitting parameters were $Z = 1.15$, $P_c = 0.03$, $\Delta = 1.4$ meV (see text for details).

polarization, however, is well below the usually reported current polarization of Ni.

C. Generalization of BTK model for a ferromagnetic electrode (Model II)

We next introduce ferromagnetism through an exchange splitting J in one of the electrodes. Therefore wave-vectors depend on spin as $\hbar k_\sigma = (2m(E_F + \sigma J/2))^{1/2}$. Transmission across the barrier is therefore spin-dependent, and Andreev reflection mixes both spins, giving different normal and Andreev reflection probabilities for each spin. Conductance can be calculated for each spin in the same way as in the BTK model using these reflection probabilities. Total conductance will be then $G = G_\uparrow + G_\downarrow$, where

$$G_\sigma = 2 e^2 v_{F\sigma} N_{F\sigma} S \int d\epsilon \left(1 + \frac{k_{-\sigma}}{k_\sigma} A_\sigma - R_\sigma \right) \frac{df(\epsilon - eV)}{d\epsilon} \quad (4)$$

The adjustable parameters in this model are J , the height of the barrier for zero splitting Z , again modeled by a delta function, and the gap at the interface Δ .

This model leads to the results shown in Fig. 4. A good fit is obtained using $Z = 1.13$, $\Delta = 1.4$ meV and $J = 0.8$ eV, which agrees well with the electronic band structure of Ni. This exchange provides a bulk polarization

$$P_b = \frac{n_\uparrow - n_\downarrow}{n_\uparrow + n_\downarrow} \approx \frac{J}{2E_F} \approx 0.4 \quad (5)$$

if we take $E_F \simeq 1$ eV, which is the bottom of the band of Ni along our experimental FL direction. The model also

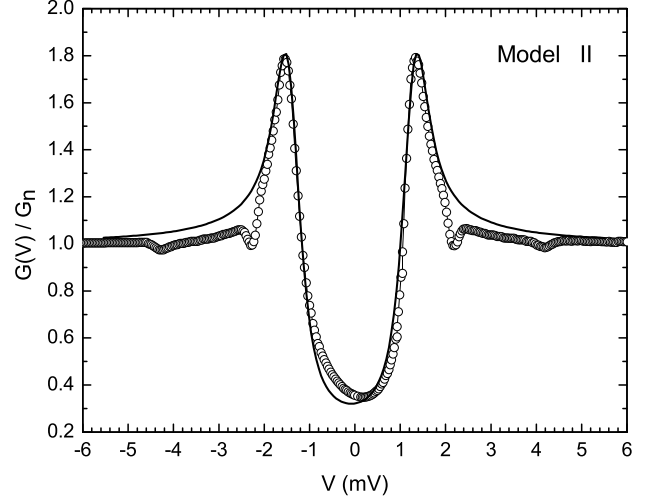


FIG. 4: Fit to the experimental results obtained with model II (see text for details). The fitting parameters were $Z = 1.13$, $\Delta = 1.4$ meV, $J = 0.8$ eV and the transmission coefficients were $T_\uparrow = 0.48$ and $T_\downarrow = 0.37$.

allows us to define the current polarization, assuming a unidimensional barrier, in terms of the difference in the transmission coefficients through the barrier, $T_\uparrow = 0.48$ and $T_\downarrow = 0.37$. We find

$$P_c \approx \frac{T_\uparrow - T_\downarrow}{T_\uparrow + T_\downarrow} \approx 0.13, \quad (6)$$

which we still feel to be somewhat too low.

We note that the polarization as determined from the transmission coefficients needs not agree with the bulk polarization of the ferromagnetic electrode.^{16,17} Similar effects can arise when the conduction bands are built up of localized and delocalized atomic orbitals.¹⁸ A comparison between the polarization defined using Eq.(6) and the bulk polarization, for barrier strengths in the range from 0.2 to 3.5 is shown in Fig. 5. In the limits $P_b \rightarrow 0$ and $P_b \rightarrow 1$ both polarizations are equal, but for intermediate values current polarization is always smaller than bulk one.

D. Simple quasiclassical theory (Model III)

We now use quasiclassical theory, with boundary conditions dumped into the transmission coefficients T_σ . Conductance is then determined using Eq. (4) with $k_\uparrow = k_\downarrow$, where the effective reflection coefficients are

$$A_\sigma = T_\sigma T_{-\sigma} \left| \frac{f}{1 + r_\sigma r_{-\sigma} + (1 - r_\sigma r_{-\sigma}) g} \right|^2$$

$$R_\sigma = \left| \frac{r_\sigma + r_{-\sigma} + (r_\sigma - r_{-\sigma}) g}{1 + r_\sigma r_{-\sigma} + (1 - r_\sigma r_{-\sigma}) g} \right|^2. \quad (7)$$

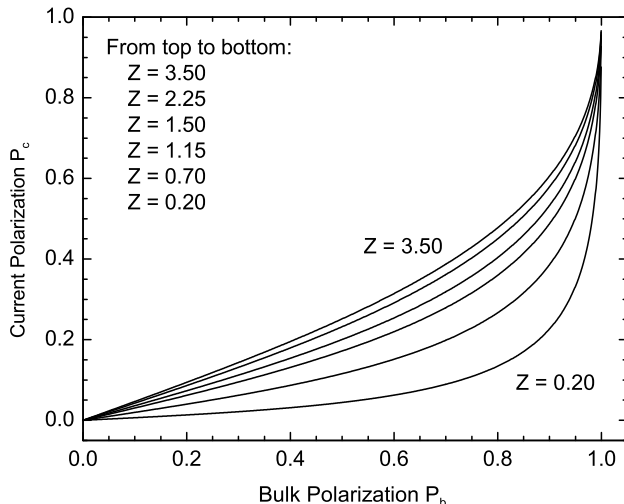


FIG. 5: Polarization determined from the transmission coefficients across the barrier, eq.(6) as a function of the bulk polarization of the ferromagnetic electrode.

Here g and f are the (spin independent) normal and anomalous components of the Green's functions evaluated right at the interface, at the superconducting side, and $r_\sigma^2 + T_\sigma = 1$.

This scheme is, in principle, exact, although it does not allow us to extract information about the nature of the barrier, which is treated as a black box whose internal structure is ignored. We also assume that the electrodes are in the clean limit, to simplify the calculation. Once the transmission coefficients across the barrier which best fit the experimental data have been determined, we have performed calculations in the normal regime with more realistic square barriers in order to check the physical properties of the model. Neglecting effects related to the dispersion in the direction parallel to the junction, the results obtained using this model should be reproduced by the generalized BTK model with the appropriate choice of transmission coefficients.

The best results obtained using this model are shown in Fig. 6. The parameters used are $\Delta = 1.38$ meV, $T_\uparrow = 0.5$ and $T_\downarrow = 0.32$. Using the expression in eq.(6) we obtain a current polarization $P_c = 0.22$.

E. Characterization of the barrier

We have also related the transmission coefficients used in the fits with the thickness d and height U of more realistic square barriers. Grundner and Halbritter have found that the effective height of the barrier of Nb_2O_5 oxide layers is of order $U \approx 0.1$ eV.¹⁰ Fig. 7 shows the transmission through a barrier of such height as function of d , for different values of bulk polarization. The Fermi energy in the Ni ferromagnetic electrode is approximately $E_F \approx 1$ eV, while in the Nb superconducting electrode is

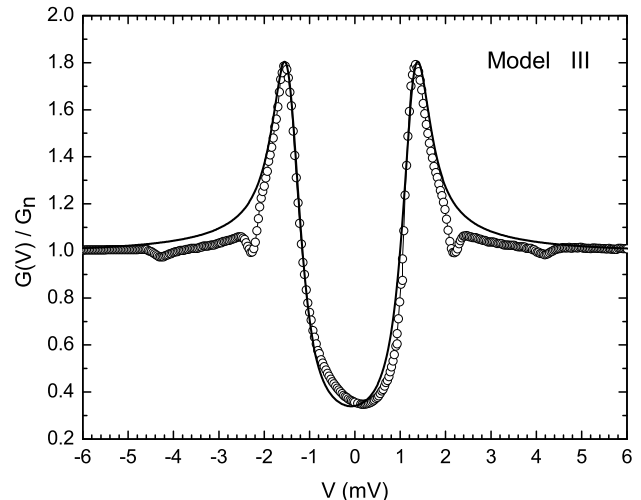


FIG. 6: Fit to the experimental results obtained with model III (see text for details). The fitting parameters were $\Delta = 1.38$ meV and the used transmission coefficients were $T_\uparrow = 0.5$ and $T_\downarrow = 0.32$.

of about $E_F \approx 1.5$ eV along the ΓP direction. We find transmission coefficients comparable to those required to fit the experimental data for barrier depths $d \sim 5$ Å.

The significant conductance observed at voltages below the gap implies the existence of good contacts. One may get an estimate of the number of these contacts by dividing the quantum unit of resistance, $h/(2e^2)$ by the observed resistance, $R = 20 \Omega$ (the fact that the transmission coefficients needed to fit the data are below 1 does not alter the order of magnitude). Assuming that the area of each of these conducting channels is of the order of a few tens of Å² we obtain that the area of these contacts is a small fraction of the area of the oxide barrier (10^{-8}), suggesting that the conductance is mainly due to tiny spots where the barrier is narrower than the average thickness of the oxide layer. The existence of zones where the barrier is ~ 5 Å thick is not inconsistent with the experimentally observed corrugation, and agrees with our estimation of the barrier depth.

IV. SUMMARY AND CONCLUSIONS

The experimental results can be fit with different models. The simplest one, which describes the junction in terms of a paramagnetic and a fully polarized channel, requires as an input a bulk polarization which is much lower than the observed polarization of Ni. A more accurate one is the exact generalization of the BTK model, which describes properly the bulk polarization of Ni but not its current one. A scattering approach, which does not require knowledge of the structure of the barrier, describes well the experimental data with reasonable values for the transmission coefficients for majority and minority spins,

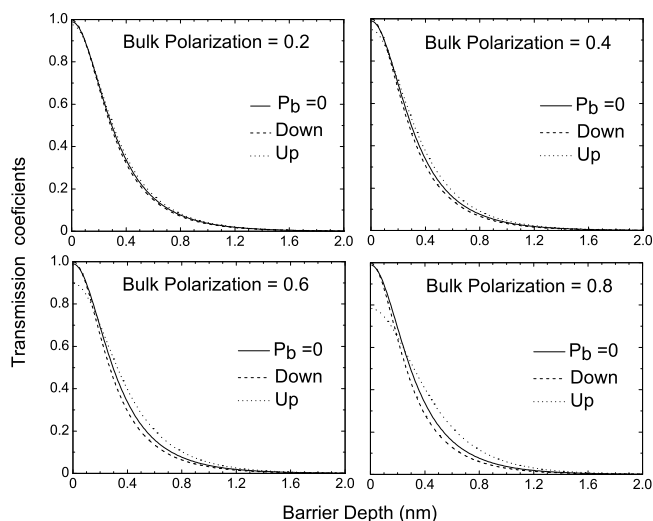


FIG. 7: Transmission coefficients as a function of barrier depth for a barrier of height $U = 0.1$ eV. Bulk polarization in the ferromagnetic electrode is, from left to right and from top to bottom: 0.2, 0.4, 0.6, 0.8, as indicated in each graph.

giving the correct value of the current polarization. The

experimental data show an additional contribution which is not symmetric with respect to the applied voltage, this small asymmetry is not relevant for our results. This contribution may arise from inelastic scattering of magnons at the interface.¹⁹

The polarization inferred from the transmission coefficients calculated with the BTK model does not coincide with the bulk magnetization of the ferromagnetic electrode, used as an input. We have studied the relation between these two quantities, showing a significant dependence on the height of the barrier.

Acknowledgments

This work was supported by C.I.C.Y.T. (MAT2002-04543, MAT 2002-02219, MAT2002-0495-C02-01, BFM2003-03156) and Ramón Areces Foundation. E.M.G. acknowledges Ministerio de Ciencia y Tecnología for a Ramón y Cajal contract. A.D.-F. thanks Ministerio de Educación, Cultura y Deporte for a FPU grant (AP2002-1383). R. Escudero thanks Universidad Complutense and Ministerio de Educación, Cultura y Deporte for a sabbatical professorship.

* On leave from Instituto de Investigación en Materiales, Universidad Nacional Autónoma de México, México D. F.

¹ J. E. Christopher, R. V. Coleman, A. Isin, and R. C. Morris, *Phys. Rev. B* **172**, 485 (1968).

² B. J. Jonsson-Akerman, R. Escudero, C. Leighton, and Ivan K. Schuller, *Appl. Phys. Lett.* **77**, 1870 (2000)

³ G. Prinz, *Phys. Today* **48**, 58 (1995).

⁴ J. de Boeck, *Science* **281**, 357 (1998).

⁵ R. Meservey and P. M. Tedrow, *Phys. Rep.* **238**, 173 (1994).

⁶ S. K. Upadhyay, A. Palanisami, R. N. Louie, and R. A. Buhrman, *Phys. Rev. Lett.* **81**, 3247 (1998).

⁷ R. J. Soulen Jr., J. M. Byers, M. S. Osofsky, B. Nadgorny, T. Ambrose, S. F. Chen, P. R. Broussard, C. T. Tanaka, J. Nowak, J. S. Moodera, A. Barry, and J. M. D. Coey, *Science* **282**, 85 (1998).

⁸ T. H. Kim, and J. S. Moodera, *Phys. Rev. B* **69**, 020403(R) (2004).

⁹ J. E. Villegas, E. Navarro, D. Jaque, E. M. González, J. I. Martín, and J. L. Vicent, *Physica C* **369**, 213 (2002).

¹⁰ M. Grundner and J. Halbritter, *Surface Science* **136**, 144 (1984).

¹¹ E. E. Fullerton, I. K. Schuller, H. Vanderstraeten, and Y. Bruynseraede, *Phys. Rev. B* **45**, 9292 (1992).

¹² G. E. Blonder, M. Tinkham, and T. M. Klapwijk, *Phys. Rev. B* **25**, 4515 (1982).

¹³ G. J. Strijkers, Y. Ji, F. Y. Yang, C. L. Chien, and J. M. Byers, *Phys. Rev. B* **63**, 104510 (2001).

¹⁴ Y. Ji, G. J. Strijkers, F. Y. Yang, and C. L. Chien, *Phys. Rev. B* **64**, 224425 (2001).

¹⁵ F. Pérez-Willard, J. Cuevas, C. Suergers, P. Pfundstein, J. K. M. Eschring, and H. v. Loehneysen, *cond-mat/0306241*.

¹⁶ J. M. MacLaren, X.-G. Zhang, and W. H. Butler, *Phys. Rev. B* **56**, 11827 (1997).

¹⁷ I. I. Mazin, *Phys. Rev. Lett.* **83**, 1427 (1999).

¹⁸ J. M. D. Teresa, A. Barthelemy, A. Fert, J. P. Contour, F. Montaigne, and P. Seneor, *Science* **286**, 507 (1999).

¹⁹ G. Tkachov, E. McCann, and V. I. Falko, *Phys. Rev. B* **65**, 024519 (2001).